PHYSICAL REVIEW C **77**, 061902(R) (2008)

# Spin alignment measurements of the $K^{*0}(892)$ and $\phi(1020)$ vector mesons in heavy ion collisions at $\sqrt{s_{NN}} = 200$ GeV

B. I. Abelev,[10] M. M. Aggarwal,[32] Z. Ahammed,[47] B. D. Anderson,[21] D. Arkhipkin,[14] G. S. Averichev,[13] Y. Bai,[30] J. Balewski,[25] O. Barannikova,[10] L. S. Barnby,[2] J. Baudot,[19] S. Baumgart,[52] D. R. Beavis,[3] R. Bellwied,[50] F. Benedosso,[30] R. R. Betts,[10] S. Bhardwaj,[37] A. Bhasin,[20] A. K. Bhati,[32] H. Bichsel,[49] J. Bielcik,[12] J. Bielcikova,[12] B. Biritz,[7] L. C. Bland,[3] M. Bombara,[2] B. E. Bonner,[38] M. Botje,[30] J. Bouchet,[21] E. Braidot,[30] A. V. Brandin,[28] S. Bueltmann,[3] T. P. Burton,[2] M. Bystersky,[12] X. Z. Cai,[41] H. Caines,[52] M. Calderón de la Barca Sánchez,[6] J. Callner,[10] O. Catu,[52] D. Cebra,[6] R. Cendejas,[7] M. C. Cervantes,[43] Z. Chajecki,[31] P. Chaloupka,[12] S. Chattopadhyay,[47] H. F. Chen,[40] J. H. Chen,[41] J. Y. Chen,[51] J. Cheng,[45] M. Cherney,[11] A. Chikanian,[52] K. E. Choi,[36] W. Christie,[3] S. U. Chung,[3] R. F. Clarke,[43] M. J. M. Codrington,[43] J. P. Coffin,[19] T. M. Cormier,[50] M. R. Cosentino,[39] J. G. Cramer,[49] H. J. Crawford,[5] D. Das,[6] S. Dash,[16] M. Daugherity,[44] M. M. de Moura,[39] T. G. Dedovich,[13] M. DePhillips,[3] A. A. Derevschikov,[34] R. Derradi de Souza,[8] L. Didenko,[3] T. Dietel,[15] P. Djawotho,[18] S. M. Dogra,[20] X. Dong,[24] J. L. Drachenberg,[43] J. E. Draper,[6] F. Du,[52] J. C. Dunlop,[3] M. R. Dutta Mazumdar,[47] W. R. Edwards,[24] L. G. Efimov,[13] E. Elhalhuli,[2] M. Elnimr,[50] V. Emelianov,[28] J. Engelage,[5] G. Eppley,[38] B. Erazmus,[42] M. Estienne,[19] L. Eun,[33] P. Fachini,[3] R. Fatemi,[22] J. Fedorisin,[13] A. Feng,[51] P. Filip,[14] E. Finch,[52] V. Fine,[3] Y. Fisyak,[3] C. A. Gagliardi,[43] L. Gaillard,[2] D. R. Gangadharan,[7] M. S. Ganti,[47] E. Garcia-Solis,[10] V. Ghazikhanian,[7] P. Ghosh,[47] Y. N. Gorbunov,[11] A. Gordon,[3] O. Grebenyuk,[30] D. Grosnick,[46] B. Grube,[36] S. M. Guertin,[7] K. S. F. F. Guimaraes,[39] A. Gupta,[20] N. Gupta,[20] W. Guryn,[3] B. Haag,[6] T. J. Hallman,[3] A. Hamed,[43] J. W. Harris,[52] W. He,[18] M. Heinz,[52] S. Heppelmann,[33] B. Hippolyte,[19] A. Hirsch,[35] A. M. Hoffman,[25] G. W. Hoffmann,[44] D. J. Hofman,[10] R. S. Hollis,[10] H. Z. Huang,[7] E. W. Hughes,[4] T. J. Humanic,[31] G. Igo,[7] A. Iordanova,[10] P. Jacobs,[24] W. W. Jacobs,[18] P. Jakl,[12] F. Jin,[41] P. G. Jones,[2] E. G. Judd,[5] S. Kabana,[42] K. Kajimoto,[44] K. Kang,[45] J. Kapitan,[12] M. Kaplan,[9] D. Keane,[21] A. Kechechyan,[13] D. Kettler,[49] V. Yu. Khodyrev,[34] J. Kiryluk,[24] A. Kisiel,[31] S. R. Klein,[24] A. G. Knospe,[52] A. Kocoloski,[25] D. D. Koetke,[46] T. Kollegger,[15] M. Kopytine,[21] L. Kotchenda,[28] V. Kouchpil,[12] P. Kravtsov,[28] V. I. Kravtsov,[34] K. Krueger,[1] C. Kuhn,[19] A. Kumar,[32] L. Kumar,[32] P. Kurnadi,[7] M. A. C. Lamont,[3] J. M. Landgraf,[3] S. Lange,[15] S. LaPointe,[50] F. Laue,[3] J. Lauret,[3] A. Lebedev,[3] R. Lednicky,[14] C-H. Lee,[36] M. J. LeVine,[3] C. Li,[40] Y. Li,[45] G. Lin,[52] X. Lin,[51] S. J. Lindenbaum,[29] M. A. Lisa,[31] F. Liu,[51] H. Liu,[40] J. Liu,[38] L. Liu,[51] T. Ljubicic,[3] W. J. Llope,[38] R. S. Longacre,[3] W. A. Love,[3] Y. Lu,[40] T. Ludlam,[3] D. Lynn,[3] G. L. Ma,[41] J. G. Ma,[7] Y. G. Ma,[41] D. P. Mahapatra,[16] R. Majka,[52] L. K. Mangotra,[20] R. Manweiler,[46] S. Margetis,[21] C. Markert,[44] H. S. Matis,[24] Yu. A. Matulenko,[34] T. S. McShane,[11] A. Meschanin,[34] J. Millane,[25] M. L. Miller,[25] N. G. Minaev,[34] S. Mioduszewski,[43] A. Mischke,[30] J. Mitchell,[38] B. Mohanty,[47] D. A. Morozov,[34] M. G. Munhoz,[39] B. K. Nandi,[17] C. Nattrass,[52] T. K. Nayak,[47] J. M. Nelson,[2] C. Nepali,[21] P. K. Netrakanti,[35] M. J. Ng,[5] L. V. Nogach,[34] S. B. Nurushev,[34] G. Odyniec,[24] A. Ogawa,[3] H. Okada,[3] V. Okorokov,[28] D. Olson,[24] M. Pachr,[12] S. K. Pal,[47] Y. Panebratsev,[13] T. Pawlak,[48] T. Peitzmann,[30] V. Perevoztchikov,[3] C. Perkins,[5] W. Peryt,[48] S. C. Phatak,[16] M. Planinic,[53] J. Pluta,[48] N. Poljak,[53] N. Porile,[35] A. M. Poskanzer,[24] M. Potekhin,[3] B. V. K. S. Potukuchi,[20] D. Prindle,[49] C. Pruneau,[50] N. K. Pruthi,[32] J. Putschke,[52] I. A. Qattan,[18] R. Raniwala,[37] S. Raniwala,[37] R. L. Ray,[44] A. Ridiger,[28] H. G. Ritter,[24] J. B. Roberts,[38] O. V. Rogachevskiy,[13] J. L. Romero,[6] A. Rose,[24] C. Roy,[42] L. Ruan,[3] M. J. Russcher,[30] V. Rykov,[21] R. Sahoo,[42] I. Sakrejda,[24] T. Sakuma,[25] S. Salur,[24] J. Sandweiss,[52] M. Sarsour,[43] J. Schambach,[44] R. P. Scharenberg,[35] N. Schmitz,[26] J. Seger,[11] I. Selyuzhenkov,[18] P. Seyboth,[26] A. Shabetai,[19] E. Shahaliev,[13] M. Shao,[40] M. Sharma,[50] S. S. Shi,[51] X-H. Shi,[41] E. P. Sichtermann,[24] F. Simon,[26] R. N. Singaraju,[47] M. J. Skoby,[35] N. Smirnov,[52] R. Snellings,[30] P. Sorensen,[3] J. Sowinski,[18] H. M. Spinka,[1] B. Srivastava,[35] A. Stadnik,[13] T. D. S. Stanislaus,[46] D. Staszak,[7] R. Stock,[15] M. Strikhanov,[28] B. Stringfellow,[35] A. A. P. Suaide,[39] M. C. Suarez,[10] N. L. Subba,[21] M. Sumbera,[12] X. M. Sun,[24] Z. Sun,[23] B. Surrow,[25] T. J. M. Symons,[24] A. Szanto de Toledo,[39] J. Takahashi,[8] A. H. Tang,[3] Z. Tang,[40] T. Tarnowsky,[35] D. Thein,[44] J. H. Thomas,[24] J. Tian,[41] A. R. Timmins,[2] S. Timoshenko,[28] M. Tokarev,[13] T. A. Trainor,[49] V. N. Tram,[24] A. L. Trattner,[5] S. Trentalange,[7] R. E. Tribble,[43] O. D. Tsai,[7] J. Ulery,[35] T. Ullrich,[3] D. G. Underwood,[1] G. Van Buren,[3] N. van der Kolk,[30] M. van Leeuwen,[30] A. M. Vander Molen,[27] R. Varma,[17] G. M. S. Vasconcelos,[8] I. M. Vasilevski,[14] A. N. Vasiliev,[34] F. Videbaek,[3] S. E. Vigdor,[18] Y. P. Viyogi,[16] S. Vokal,[13] S. A. Voloshin,[50] M. Wada,[44] W. T. Waggoner,[11] F. Wang,[35] G. Wang,[7] J. S. Wang,[23] Q. Wang,[35] X. Wang,[45] X. L. Wang,[40] Y. Wang,[45] J. C. Webb,[46] G. D. Westfall,[27] C. Whitten Jr.,[7] H. Wieman,[24] S. W. Wissink,[18] R. Witt,[52] J. Wu,[40] Y. Wu,[51] N. Xu,[24] Q. H. Xu,[24] Z. Xu,[3] P. Yepes,[38] I-K. Yoo,[36] Q. Yue,[45] M. Zawisza,[48] H. Zbroszczyk,[48] W. Zhan,[23] H. Zhang,[3] S. Zhang,[41] W. M. Zhang,[21] Y. Zhang,[40] Z. P. Zhang,[40] Y. Zhao,[40] C. Zhong,[41] J. Zhou,[38] R. Zoulkarneev,[14] Y. Zoulkarneeva,[14] and J. X. Zuo[41]

(STAR Collaboration)

[1]*Argonne National Laboratory, Argonne, Illinois 60439, USA*

[2]*University of Birmingham, Birmingham, United Kingdom*

[3]*Brookhaven National Laboratory, Upton, New York 11973, USA*

[4]*California Institute of Technology, Pasadena, California 91125, USA*

[5]*University of California, Berkeley, California 94720, USA*

[6]*University of California, Davis, California 95616, USA*

[7]*University of California, Los Angeles, California 90095, USA*

[8]*Universidade Estadual de Campinas, Sao Paulo, Brazil*

 

[9]*Carnegie Mellon University, Pittsburgh, Pennsylvania 15213, USA*
[10]*University of Illinois at Chicago, Chicago, Illinois 60607, USA*
[11]*Creighton University, Omaha, Nebraska 68178, USA*
[12]*Nuclear Physics Institute AS CR, 250 68 Řež / Prague, Czech Republic*
[13]*Laboratory for High Energy (JINR), Dubna, Russia*
[14]*Particle Physics Laboratory (JINR), Dubna, Russia*
[15]*University of Frankfurt, Frankfurt, Germany*
[16]*Institute of Physics, Bhubaneswar 751005, India*
[17]*Indian Institute of Technology, Mumbai, India*
[18]*Indiana University, Bloomington, Indiana 47408, USA*
[19]*Institut de Recherches Subatomiques, Strasbourg, France*
[20]*University of Jammu, Jammu 180001, India*
[21]*Kent State University, Kent, Ohio 44242, USA*
[22]*University of Kentucky, Lexington, Kentucky 40506-0055, USA*
[23]*Institute of Modern Physics, Lanzhou, People's Republic of China*
[24]*Lawrence Berkeley National Laboratory, Berkeley, California 94720, USA*
[25]*Massachusetts Institute of Technology, Cambridge, Massachusetts 02139-4307, USA*
[26]*Max-Planck-Institut für Physik, Munich, Germany*
[27]*Michigan State University, East Lansing, Michigan 48824, USA*
[28]*Moscow Engineering Physics Institute, Moscow Russia*
[29]*City College of New York, New York City, New York 10031, USA*
[30]*NIKHEF and Utrecht University, Amsterdam, The Netherlands*
[31]*Ohio State University, Columbus, Ohio 43210, USA*
[32]*Panjab University, Chandigarh 160014, India*
[33]*Pennsylvania State University, University Park, Pennsylvania 16802, USA*
[34]*Institute of High Energy Physics, Protvino, Russia*
[35]*Purdue University, West Lafayette, Indiana 47907, USA*
[36]*Pusan National University, Pusan, Republic of Korea*
[37]*University of Rajasthan, Jaipur 302004, India*
[38]*Rice University, Houston, Texas 77251, USA*
[39]*Universidade de Sao Paulo, Sao Paulo, Brazil*
[40]*University of Science & Technology of China, Hefei 230026, People's Republic of China*
[41]*Shanghai Institute of Applied Physics, Shanghai 201800, People's Republic of China*
[42]*SUBATECH, Nantes, France*
[43]*Texas A&M University, College Station, Texas 77843, USA*
[44]*University of Texas, Austin, Texas 78712, USA*
[45]*Tsinghua University, Beijing 100084, People's Republic of China*
[46]*Valparaiso University, Valparaiso, Indiana 46383, USA*
[47]*Variable Energy Cyclotron Centre, Kolkata 700064, India*
[48]*Warsaw University of Technology, Warsaw, Poland*
[49]*University of Washington, Seattle, Washington 98195, USA*
[50]*Wayne State University, Detroit, Michigan 48201, USA*
[51]*Institute of Particle Physics, CCNU (HZNU), Wuhan 430079, People's Republic of China*
[52]*Yale University, New Haven, Connecticut 06520, USA*
[53]*University of Zagreb, Zagreb, HR-10002, Croatia*

(Received 11 January 2008; published 12 June 2008)

We present the first spin alignment measurements for the $K^{*0}(892)$ and $\phi(1020)$ vector mesons produced at midrapidity with transverse momenta up to 5 GeV/$c$ at $\sqrt{s_{NN}} = 200$ GeV at RHIC. The diagonal spin-density matrix elements with respect to the reaction plane in Au + Au collisions are $\rho_{00} = 0.32 \pm 0.04$ (stat) $\pm$ 0.09 (syst) for the $K^{*0}$ ($0.8 < p_T < 5.0$ GeV/$c$) and $\rho_{00} = 0.34 \pm 0.02$ (stat) $\pm$ 0.03 (syst) for the $\phi$ ($0.4 < p_T < 5.0$ GeV/$c$) and are constant with transverse momentum and collision centrality. The data are consistent with the unpolarized expectation of 1/3 and thus no evidence is found for the transfer of the orbital angular momentum of the colliding system to the vector-meson spins. Spin alignments for $K^{*0}$ and $\phi$ in Au + Au collisions were also measured with respect to the particle's production plane. The $\phi$ result, $\rho_{00} = 0.41 \pm 0.02$ (stat) $\pm 0.04$ (syst), is consistent with that in $p+p$ collisions, $\rho_{00} = 0.39 \pm 0.03$ (stat) $\pm 0.06$ (syst), also measured in this work. The measurements thus constrain the possible size of polarization phenomena in the production dynamics of vector mesons.

DOI: 10.1103/PhysRevC.77.061902 PACS number(s): 24.70.+s, 25.75.Nq

Measurements of the polarization of the particles produced in relativistic heavy-ion collisions may provide new insights into the initial conditions and evolution of the nuclear system during the collision [1–3]. In particular, by studying the polarization magnitudes with respect to various kinematic planes one could attempt to discern the point in the evolution of the system at which the polarization arises and, hence, the dominant mechanisms involved. The planes that are relevant to this Rapid Communication are the reaction plane, which is defined by the beam momentum and the nuclear impact parameter, and the particle's production plane, which is defined by the beam momentum and the momentum of the produced particle.

In noncentral relativistic heavy-ion collisions, transverse gradients of the total longitudinal momentum of the participant matter result in substantial local orbital angular momentum of the created partons [1]. Due to the spin-orbit coupling of quantum chromodynamics (QCD), this orbital motion may result in a net polarization of the produced particles along the direction of the initial angular momentum, that is, perpendicular to the reaction plane, yielding a global hadronic polarization in the final state [1,4,5]. The magnitude and the transverse-momentum ($p_T$) dependence of the global polarization are therefore expected to be sensitive to different hadronization scenarios [6]. In particular, the proposed quark recombination model for hadronization of bulk partonic matter created at RHIC [7], which reproduces measurements in the intermediate $p_T$ region ($2 < p_T < 5$ GeV/$c$) quite well [8], may be an effective dynamical mechanism for transferring polarization from quarks to vector mesons or hyperons.

One can study the polarization of final-state hadrons with respect to the particle's production plane as well. Nonzero polarizations transverse to this plane are expected to be sensitive to particle formation dynamics and to possible intrinsic quark transverse spin distributions [9]. Because large production plane polarizations have been observed for hyperons in unpolarized $p+p$ and $p+A$ interactions [10] and for vector mesons in $K+p, n+C$, and $e^+e^-$ interactions [11–14], the disappearance of these effects in relativistic heavy-ion collisions might indicate that the system is isotropic to the extent that, locally, there is no longer a preferred direction [15]. It has also been suggested [16] that vector-meson spin alignment with respect to the production plane is closely related to the single-spin left-right asymmetries in transversely polarized $p+p$ collisions [17–20].

We have recently measured the global (reaction plane) polarizations of $\Lambda$ and $\bar{\Lambda}$ hyperons produced at midrapidity in Au + Au collisions at center-of-mass energies $\sqrt{s_{NN}} =$ 62.4 GeV and 200 GeV [21]. The results, $|P_{\Lambda,\bar{\Lambda}}| \leqslant 0.02$, are well below the predictions of Ref. [1] and are in agreement with the refined calculations of Ref. [4].

In this Rapid Communication, we present the first measurements of the spin alignment for the $K^{*0}$ and $\phi$ vector mesons with respect to both the reaction plane and the production plane in Au + Au collisions at $\sqrt{s_{NN}} = 200$ GeV. We present also the spin alignment of the $\phi$ meson with respect to its production plane for $p+p$ collisions at the same collision energy. The $K^{*0}$ data cover $0.8 < p_T < 5.0$ GeV/$c$ and the $\phi$ data cover $0.4 < p_T < 5.0$ GeV/$c$.

Spin alignment is described by a spin-density matrix $\rho$, a $3 \times 3$ Hermitian matrix with unit trace. A deviation of the diagonal elements $\rho_{mm} (m = -1, 0, 1)$ from 1/3 signals net spin alignment. Because vector mesons decay strongly, the diagonal elements $\rho_{-1-1}$ and $\rho_{11}$ are degenerate and $\rho_{00}$ is the only independent observable. It can be determined from the angular distribution of the decay products [22],

$$\frac{dN}{d(\cos\theta^*)} = N_0 \times [(1-\rho_{00}) + (3\rho_{00}-1)\cos^2\theta^*], \quad (1)$$

where $N_0$ is the normalization and $\theta^*$ is the angle between the polarization direction $\hat{n}$ and the momentum direction of a daughter particle in the rest frame of the parent vector meson. In the case of a global spin alignment measurement, the polarization direction $\hat{n}$ is along the orbital angular momentum of the colliding system. It is determined by the reaction plane, requiring only the second-order term because Eq. (1) is invariant under $\theta^* \to \pi + \theta^*$ [23]. For the production plane measurement, $\hat{n}$ lies along the normal to the production plane, which is determined by the momentum of the vector meson and of the colliding beams.

Vector mesons are expected to originate predominantly from primordial production [24,25], unlike hyperon production, which is expected to have large resonance decay contributions [21,24,25]. Another difference between the present spin alignment measurement and our recent measurement of global hyperon polarization [21] is that contributions to a spin alignment measurement are generally additive, whereas contributions along a polarization direction may cancel. Last, as far as the reaction plane resolution is concerned, the aforementioned method has an advantage over the method used in Ref. [21], where the reaction plane was estimated in forward detectors.

A total of approximately $2.3 \times 10^7$ events from Au + Au data collection in the year 2004 run and $6.0 \times 10^6$ events from $p+p$ data collection in the year 2001 run have been used in these analyses. The events were collected with minimum bias triggers [26,27]. Charged tracks were reconstructed with the STAR Time Projection Chamber (TPC) for pseudorapidities $|\eta| < 1.0$ and all azimuthal angles [28]. Particle identification is achieved by correlating the ionization energy loss ($dE/dx$) of charged particles in the TPC gas with their measured momenta. The measured $\langle dE/dx \rangle$ is reasonably well described by the Bichsel function smeared with a resolution of width $\sigma$ [29]. By measuring the $\langle dE/dx \rangle$, pions and kaons could be identified up to a momentum of about 0.6 GeV/$c$, whereas protons could be separated from pions and kaons up to a momentum of about 1.1 GeV/$c$. Tracks within $2\sigma$ of the pion/kaon Bichsel curve were selected in the analyses. The $K^{*0}$ and $\phi$ mesons were reconstructed through their respective hadronic decay channels, $K^{*0} \to K^+\pi^-$, $\overline{K^{*0}} \to K^-\pi^+$, and $\phi \to K^+K^-$. The $K^{*0}$ and $\overline{K^{*0}}$ samples were combined to enhance the statistics and the term $K^{*0}$ in the remainder of this Rapid Communication will refer to the combined sample. The collision centrality was determined by the charged hadron multiplicity within $|\eta| < 0.5$. The same analysis techniques have been used in our earlier measurements of $K^{*0}$ and $\phi$ production [26,27].

Figure 1 illustrates aspects of the data and analysis for particular $p_T$ bins. The top panels show the invariant mass distributions for (*a*) $K^{*0}$ and (*b*) $\phi$ candidates in midcentral (20–60%) Au + Au collisions at $\sqrt{s_{NN}} = 200$ GeV, including all values of $\cos\theta^*$. In these analyses invariant mass distributions were obtained for $K^{*0}$ and $\phi$ for each $\cos\theta^*$ and $p_T$ interval. The raw $K^{*0}$ and $\phi$ yields in each of these distributions were obtained by subtracting the corresponding combinatorial backgrounds and fitting the remaining distributions with a Breit-Wigner function plus a polynomial curve to describe the residual background. The raw yields were then corrected for detection efficiency and acceptance determined from Monte Carlo GEANT simulations [26,27]. The middle panels in Fig. 1 show the $\cos\theta^*$ distributions, after efficiency and acceptance corrections, for the (*c*)$K^{*0}$ and (*d*) $\phi$, respectively. Equation (1) was fitted to these distributions to determine $\rho_{00}(p_T)$. In the analyses, we used charged particle tracks with $0.2 < p_T < 2.0$ GeV/$c$ and pseudorapidity $|\eta| < 1.0$ originating from the primary interaction vertex to reconstruct the event plane as an estimate of the reaction plane [30]. Tracks associated with a $K^{*0}$ or a $\phi$ candidate are explicitly excluded from the event plane calculation. The results for $\rho_{00}(p_T)$ were corrected for the finite event plane resolution, which was determined by correlating two random subevents. The correction factor on $(3\rho_{00} - 1)$ is determined to be 1/0.81 in 20–60% Au + Au collisions at $\sqrt{s_{NN}} = 200$ GeV [30]. The bottom panels, Figs. 1(e)–1(g), represent the $\cos\theta^*$ distribution for $K^{*0}$ and $\phi$ mesons with respect to the production plane in Au + Au and $p+p$ collisions. In this case, $\rho_{00}(p_T)$ is extracted directly by fitting Eq. (1) to the distributions. We have checked our analysis procedure by extracting $\rho_{00}$ for the abundantly produced, but spinless $K^0_S$ meson ($J^P = 0^-$). The results are shown in Fig. 1(h) and are consistent with 1/3 within the statistical uncertainties, as expected. The $\chi^2/ndf$ value is unsatisfactory for the $K^0_S$ fit for $0.4 < p_T < 0.8$ GeV/$c$, which is indicative of point-to-point systematics. It reaches satisfactory values at larger $p_T$.

The measurements of the $K^{*0}$ and $\phi$ global spin alignment versus $p_T$ of the vector meson for midcentral Au + Au collisions at $\sqrt{s_{NN}} = 200$ GeV are presented in Fig. 2, and are summarized in Table I. Both statistical and systematic uncertainties are shown. The dominant contribution to the systematic uncertainty for the $\phi$ ($K^{*0}$) meson ranges from 0.020 (0.05) to 0.045 (0.10), originating from uncertainty in the magnitude and shape of the residual background after the subtraction of combinatorial background. This residual arises from the incomplete description of combinatorial background via the event mixing technique and from distortions to the background

TABLE I. The averaged spin-density matrix elements $\rho_{00}$ with respect to the reaction plane in midcentral Au + Au collisions at $\sqrt{s_{NN}} = 200$ GeV.

| | $K^{*0}$ | $\phi$ |
|---|---|---|
| $\rho_{00}(p_T < 2.0$ GeV/$c)$ | $0.31 \pm 0.04 \pm 0.09$ | $0.33 \pm 0.01 \pm 0.03$ |
| $\rho_{00}(p_T > 2.0$ GeV/$c)$ | $0.37 \pm 0.04 \pm 0.09$ | $0.35 \pm 0.04 \pm 0.05$ |
| $\rho_{00}(p_T < 5.0$ GeV/$c)$ | $0.32 \pm 0.03 \pm 0.09$ | $0.34 \pm 0.02 \pm 0.03$ |

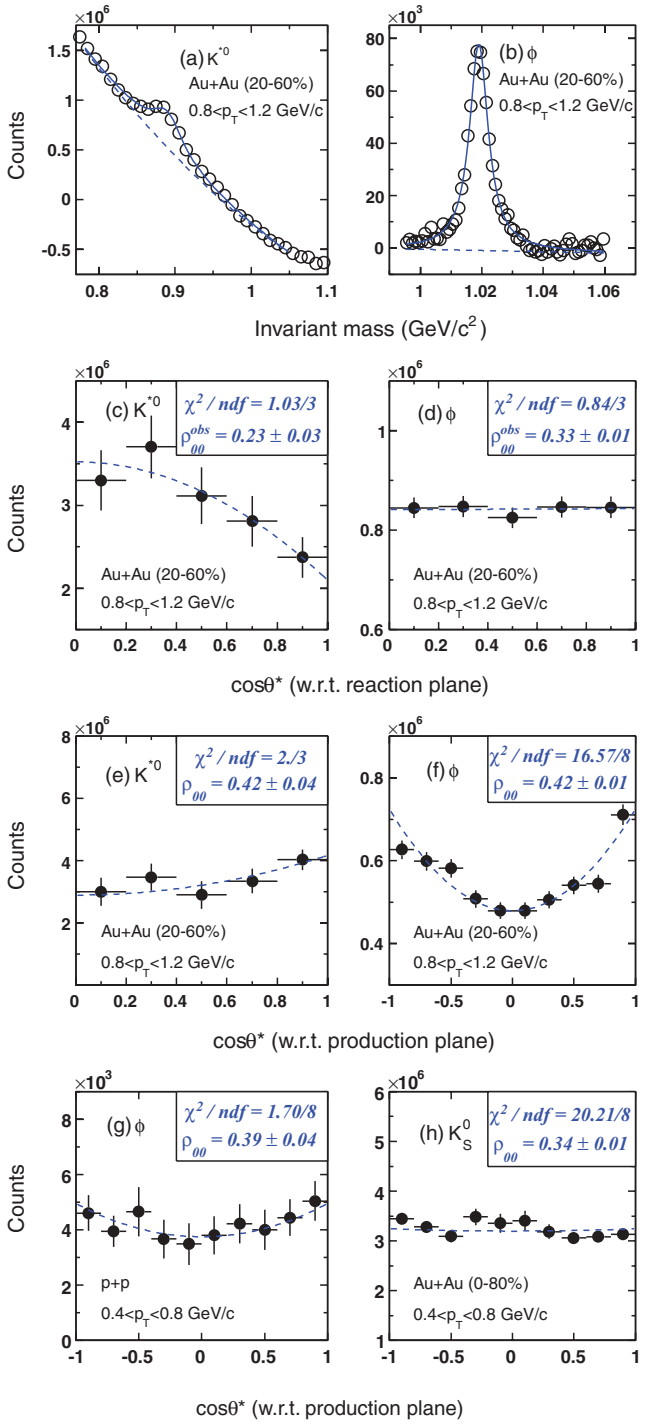


FIG. 1. (Color online) The invariant mass distribution after combinatorial background subtraction for (a) the $K^{*0}$ and (b) the $\phi$ meson in midcentral Au + Au collisions at $\sqrt{s_{NN}} = 200$ GeV, including all values of $\cos\theta^*$. The continuous lines represent fits of signal, described with a Breit-Wigner function, and residual background, described with the dashed polynomial curves. Panels (c) and (e) and panels (d) and (f) represent the $\cos\theta^*$ distributions for the $K^{*0}$ and $\phi$ yields in Au + Au collisions, respectively. Panel (g) is the $\phi$ yield in $p+p$ collisions, whereas panel (h) shows the control measurement of the spin-less $K^0_S$ meson $\cos\theta^*$ distribution. The error bars show statistical uncertainties. The blue dashed lines in (c)–(h) are fits of Eq. (1) to the data.

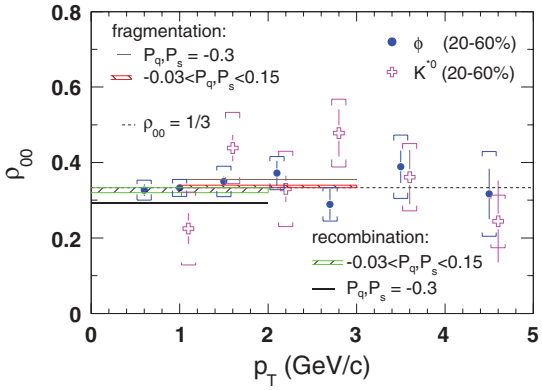


FIG. 2. (Color online) The spin-density matrix elements $\rho_{00}$ with respect to the reaction plane in midcentral Au + Au collisions at $\sqrt{s_{NN}} = 200$ GeV versus $p_T$ of the vector meson. The sizes of the statistical uncertainties are indicated by error bars, and the systematic uncertainties by caps. The $K^{*0}$ data points have been shifted slightly in $p_T$ for clarity. The dashed horizontal line indicates the unpolarized expectation $\rho_{00} = 1/3$. The bands and continuous horizontal lines show predictions discussed in the text.

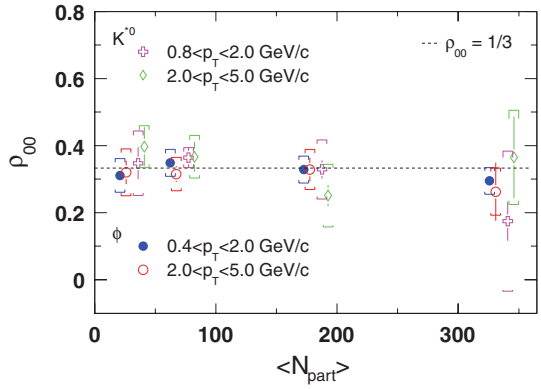


FIG. 3. (Color online) The dependence of $\rho_{00}$ with respect to the reaction plane on the number of participants at midrapidity in Au + Au collisions at $\sqrt{s_{NN}} = 200$ GeV. The sizes of the statistical uncertainties are indicated by error bars and the systematic uncertainties by caps. The $\phi$ data for $p_T > 2$ GeV/$c$ and the $K^{*0}$ data points have been shifted slightly in $\langle N_{\text{part}} \rangle$ for clarity. The dashed horizontal line indicates the unpolarized expectation $\rho_{00} = 1/3$.

in the invariant mass distribution near the $\phi$ peak caused by photon conversions and other correlated backgrounds such as $K^{0*} \to K^+\pi^-$, $\rho^0 \to \pi^+\pi^-$, $\Lambda \to p\pi^-$, and $\Delta \to N\pi$ decays [31]. In the case of the $K^{*0}$ these backgrounds include $K^0_S \to \pi^+\pi^-$, $\rho^0 \to \pi^+\pi^-$, $\phi \to K^+K^-$, $\Lambda \to p\pi^-$, and $\Delta \to N\pi$ decays [32]. Other point-to-point systematic uncertainty associated with particle identification for the $\phi$ ($K^{*0}$) meson were estimated to range from 0.007 (0.06) to 0.012 (0.09) by tightening the $K^{\pm}$ ($\pi$ and $K$) $\langle dE/dx \rangle$ cut from $2\sigma$ to $1\sigma$. An additional sizable contribution to the $\phi$ uncertainty was estimated to range from 0.007 to 0.012 by varying the fitted invariant mass range from 1.00–1.04 GeV/$c^2$ to 1.00–1.06 GeV/$c^2$ and to the $K^{*0}$ uncertainty ranging from 0.02 to 0.05 by changing its analyzed rapidity range from $|y| < 1$ to $|y| < 0.5$. The systematic uncertainties in the $K^{0*}$ measurements are larger than those in the $\phi$ measurement mainly because of the lower signal-to-background ratio of $\sim 1/1000$ compared to $\sim 1/25$ for the $\phi$ meson. The contributions to the systematic uncertainty caused by elliptic flow effects and the event plane resolution are found to be negligible. The $K^{*0}$ and $\phi$ data are consistent with each other and are consistent with 1/3 at all $p_T$.

Hadronization of globally polarized thermal quarks, typically having $p_T < 1$ GeV/$c$, in midcentral Au + Au collisions is predicted to cause $p_T$-dependent deviations of $\rho_{00}$ from the unpolarized value of 1/3 [1,4,6,33]. Recombination of polarized thermal quarks and antiquarks is expected to dominate for $p_T < 2$ GeV/$c$ and leads to values of $\rho_{00} < 1/3$ as indicated in Fig. 2 for a typical range of expected light (strange) quark polarizations $P_{q(s)}$ [6]. The fragmentation of polarized thermal quarks with larger $p_T$, however, would lead to values of $\rho_{00} > 1/3$ for $1 < p_T < 3$ GeV/$c$ [6,33], which is indicated as well. In the region of $1 < p_T < 2$ GeV/$c$ both hadronization mechanisms could occur and their effects on $\rho_{00}$ may cancel. As observed in Fig. 2 these effects are predicted to be smaller than our experiment sensitivity. However, the large (strange) quark polarization, $P_{q,s} = -0.3$, considered in the recombination scenario of Ref. [1], results in worse agreement of $\rho_{00}$ with our $\phi$ data than $-0.03 < P_{q,s} < 0.15$ discussed in Ref. [4]. Our data are consistent with the unpolarized expectation $\rho_{00} = 1/3$. Recent measurement of the $\Lambda$ and $\bar{\Lambda}$ global polarization also found no significant polarization and an upper limit, $|P_{\Lambda,\bar{\Lambda}}| \leqslant 0.02$, was obtained [21].

The centrality dependence of the global spin alignment measurements for $K^{*0}$ and $\phi$ vector mesons with low and intermediate $p_T$ is shown in Fig. 3. The orbital angular momentum of the colliding system depends strongly on the collision centrality. Global polarization is predicted to be vanishingly small in central collisions and to increase almost linearly with impact parameter in semicentral collisions due to increasing particle angular momentum along with effects of spin-orbit coupling in QCD [1]. The data exhibit no significant spin alignment at any collision centrality and thus can constrain the possible size of spin-orbit couplings.

Figure 4 and Table II present the $K^{*0}$ and $\phi$ spin alignment measurements with respect to the production plane in midcentral Au + Au collisions at $\sqrt{s_{NN}} = 200$ GeV together with the $\phi$ meson results in $p+p$ collisions at the same incident energy. As is the case for our measurements with respect to the reaction plane, the uncertainties in the measurement with respect to the production plane are smaller for the $\phi$ than for

TABLE II. The averaged spin-density matrix elements $\rho_{00}$ with respect to the production plane in midcentral Au + Au collisions and the $\phi$ result in $p+p$ collisions at $\sqrt{s_{NN}} = 200$ GeV.

| | $K^{*0}$ | $\phi$ |
|---|---|---|
| $\rho_{00}(p_T < 2.0$ GeV/$c)$ | $0.43 \pm 0.04 \pm 0.09$ | $0.42 \pm 0.02 \pm 0.04$ |
| $\rho_{00}(p_T > 2.0$ GeV/$c)$ | $0.38 \pm 0.04 \pm 0.09$ | $0.38 \pm 0.03 \pm 0.05$ |
| $\rho_{00}(p_T < 5.0$ GeV/$c)$ | $0.42 \pm 0.03 \pm 0.09$ | $0.41 \pm 0.02 \pm 0.04$ |
| $\rho_{00}$(p + p) | | $0.39 \pm 0.03 \pm 0.06$ |

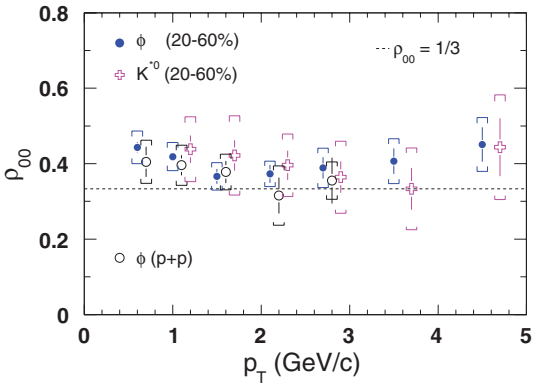


FIG. 4. (Color online) The spin-density matrix elements $\rho_{00}$ with respect to the production plane in midcentral Au + Au and $p+p$ collisions at $\sqrt{s_{NN}} = 200$ GeV versus $p_T$ of the vector meson. The sizes of the statistical uncertainties are indicated by error bars and the systematic uncertainties by caps. The $K^{*0}$ and the $\phi$ $p+p$ data points have been shifted slightly in $p_T$ for clarity. The dashed horizontal line indicates the unpolarized expectation $\rho_{00} = 1/3$.

the $K^{*0}$ meson, and the statistical uncertainties are somewhat smaller than the systematic uncertainty estimates. The $\phi$ point-to-point systematic uncertainty estimate includes a dominant contribution ranging from 0.030 to 0.045 due to residual background plus two smaller contributions of 0.006–0.012 and 0.005–0.010 estimated by varying the $K^{\pm}$ identification cut on $\langle dE/dx \rangle$ from $2\sigma$ to $1\sigma$ and the fit range of the $\phi$-meson invariant mass from 1.00–1.04 GeV/$c^2$ to 1.00–1.06 GeV/$c^2$. For the $K^{*0}$ we estimate a residual background contribution to the point-to-point systematic uncertainty ranging from 0.02 to 0.08 and about equal contributions ranging from 0.01 to 0.08 by varying particle identification criteria and analyzed rapidity. The Au + Au data for $\rho_{00}$ are consistent with 1/3 to within 1–2 times the total uncertainties, although the central values tend to increase with decreasing $p_T$ for $p_T <$ 2.0 GeV/$c$. The $p+p$ results are consistent with the Au + Au results and with 1/3. No conclusive evidence is found for large polarization phenomena in the production dynamics of vector mesons in the covered kinematic region with the precision of current measurements. The $p+p$ results are in qualitative agreement with the suggested relation of vector-meson spin alignment with respect to the production plane and the null results observed for the transverse spin asymmetries in singly polarized $p+p$ collisions at midrapidity [19,20]. OPAL and DELPHI have previously reported similar null results for the spin alignment of the $K^{*0}$ and $\phi$ mesons produced with small fractional momenta ($x_p \leqslant 0.3$, $x_p = p/p_{\text{beam}}$) in $e^+e^-$ collisions [13,14], although the production and fragmentation processes involved there are different from those at RHIC.

In summary, we have presented the first measurements of spin alignment for $K^{*0}$ and $\phi$ vector mesons at midrapidity at RHIC. The results for the diagonal spin-density matrix element $\rho_{00}$ with respect to the reaction plane in Au + Au collisions are found to be constant with $p_T$ in the measured region, covering up to 5 GeV/$c$, and constant with centrality. The data are consistent with the unpolarized expectation of 1/3 and thus provide no evidence for global spin alignment despite the large orbital angular momentum in noncentral Au + Au collisions at RHIC. The results with respect to the production plane are found to be less than 2 standard deviations above 1/3 in Au + Au collisions and are consistent with the results in $p+p$ collisions at the same collisions energy. The measurements thus constrain the possible size of polarization phenomena in the production dynamics of vector mesons. Future measurements of polarization with respect to the jet production plane are complementary to the current measurements because they are not sensitive to the initial conditions and may probe the system's mean free path [2].

We thank the RHIC Operations Group and RCF at BNL and the NERSC Center at LBNL and the resources provided by the Open Science Grid consortium for their support. This work was supported in part by the Offices of NP and HEP within the U.S. DOE Office of Science; the U.S. NSF; the Sloan Foundation; the BMBF of Germany; CNRS/IN2P3, RA, RPL, and EMN of France; EPSRC of the United Kingdom; FAPESP of Brazil; the Russian Ministry of Science and Technology; the NNSFC, CAS, MoST and MoE of China; IRP and GA of the Czech Republic; FOM of the Netherlands; DAE, DST, and CSIR of the Government of India; Swiss NSF; the Polish State Committee for Scientific Research; Slovak Research and Development Agency; and the Korea Science & Engineering Foundation.

[1] Z. T. Liang and X. N. Wang, Phys. Rev. Lett. **94**, 102301 (2005); Erratum: Phys. Rev. Lett., **96**, 039901 (2006).
[2] B. Betz, M. Gyulassy, and G. Torrieri, Phys. Rev. C **76**, 044901 (2007).
[3] F. Becattini, F. Piccinini, and J. Rizzo, Phys. Rev. C **77**, 024906 (2008).
[4] Z. Liang, J. Phys. G: Nucl. Part. Phys. **34**, S323 (2007).
[5] S. Voloshin, nucl-th/0410089.
[6] Z. Liang and X. Wang, Phys. Lett. **B629**, 20 (2005).
[7] R. Hwa and C. B. Yang, Phys. Rev. C **66**, 025205 (2002); V. Greco, C. M. Ko, and P. Levai, Phys. Rev. Lett. **90**, 202302 (2003); R. Fries, B. Muller, C. Nonaka, S. A. Bass, Phys. Rev. Lett. **90**, 202303 (2003); D. Molnar and S. A. Voloshin, Phys. Rev. Lett. **91**, 092301 (2003).
[8] J. Adams *et al.*, Nucl. Phys. **A757**, 102 (2005).
[9] B. Andersson *et al.*, Phys. Lett. **B85**, 417 (1979); J. Szwed, Phys. Lett. **B105**, 403 (1981); L. Pondrom, Phys. Rep. **122**, 57 (1985); R. Barni *et al.*, Phys. Lett. **B296**, 251 (1992); J. Soffer and N. A. Tornqvist, Phys. Rev. Lett. **68**, 907 (1992).
[10] G. Bunce *et al.*, Phys. Rev. Lett. **36**, 1113 (1976); P. T. Cox *et al.*, Phys. Rev. Lett. **46**, 877 (1981); R. Rameika *et al.*, Phys. Rev. D **33**, 3172 (1986); C. Wilkinson *et al.*, Phys. Rev. Lett. **58**, 855 (1987);L. H. Trost *et al.*, Phys. Rev. D **40**, 1703 (1989); J. Duryea *et al.*, Phys. Rev. Lett. **67**, 1193 (1991).
[11] I. Ajinenko *et al.*, Z. Phys. C **5**, 177 (1980); M. Barth *et al.*, Nucl. Phys. **B223**, 296 (1983).
[12] A. N. Aleev *et al.*, Phys. Lett. **B485**, 334 (2000).
[13] P. Abreu *et al.*, Phys. Lett. **B406**, 271 (1997).

[14] K. Ackerstaff *et al*., Phys. Lett. **B412**, 210 (1997); Z. Phys. C **74**, 437 (1997).
[15] R. Stock *et al*., *Proceeding of the Conference on Quark Matter Formation and Heavy Ion Collisions*, edited by M. Jacob and H. Satz (World Scientific, Singapore, 1982), pp. 557–582; A. D. Panagiotou, Phys. Rev. C **33**, 1999 (1986); A. Ayala, E. Cuautle, G. Herrera, and L. M. Montano, Phys. Rev. C **65**, 024902 (2002); A. Ya. Berdnikov *et al*., Acta Phys. Hung. **A22**, 139 (2005).
[16] Q. H. Xu and Z. T. Liang, Phys. Rev. D **68**, 034023 (2003).
[17] A. Bravar *et al*., Phys. Rev. Lett. **77**, 2626 (1996).
[18] J. Adams *et al*., Phys. Rev. Lett. **92**, 171801 (2004).
[19] S. S. Adler *et al*., Phys. Rev. Lett. **95**, 202001 (2005).
[20] B. I. Abelev *et al*., Phys. Rev. Lett. **99**, 142003 (2007).
[21] B. I. Abelev *et al*., Phys. Rev. C **76**, 024915 (2007).
[22] K. Schilling *et al*., Nucl. Phys. **B15**, 397 (1970); Erratum: Nucl. Phys., **B18**, 332 (1970).
[23] A. M. Poskanzer and S. A. Voloshin, Phys. Rev. C **58**, 1671 (1998).
[24] Y. J. Pei, hep-ph/9703243; Y. J. Pei, Z. Phys. C **72**, 39 (1996).
[25] F. Becattini and U. W. Heinz, Z. Phys. C **76**, 269 (1997).
[26] J. Adams *et al*., Phys. Rev. C **71**, 064902 (2005).
[27] J. Adams *et al*., Phys. Lett. **B612**, 181 (2005).
[28] M. Anderson *et al*., Nucl. Instrum. Methods A **499**, 659 (2003).
[29] H. Bichsel, Nucl. Instrum. Methods A **562**, 154 (2006).
[30] J. Adams *et al*., Phys. Rev. Lett. **95**, 122301 (2005), and references therein.
[31] J. Ma, Ph.D. thesis, University of California-Los Angeles, 2006.
[32] H. Zhang, Ph.D. thesis, Yale University, 2003.
[33] Z. Liang and X. Wang (private communication, 2007).